Interlayer coherence in superconductor bilayers

Igor V. Blinov [*] and Allan H. MacDonald
Department of Physics, The University of Texas at Austin, Austin, Texas 78712, USA

(Received 18 April 2022; revised 31 October 2022; accepted 16 November 2022; published 8 December 2022)

We investigate the possibility and implications of interlayer coherence in electrically isolated superconducting bilayers. We find that in a mean-field approximation bilayers can have superconducting and excitonic order simultaneously if repulsive interactions between layers are sufficiently strong. The excitonic order implies interlayer phase coherence and can be studied in a representation of symmetric and antisymmetric bilayer states. When both orders are present we find several solutions of the mean-field equations with different values of the the symmetric and antisymmetric state pair amplitudes. The mixed state necessarily has nonzero pair amplitudes for electrons in different layers in spite of the repulsive interlayer interactions, and these are responsible for spatially indirect Andreev reflection processes in which an incoming electron in one layer can be reflected as a hole in the opposite layer. We evaluate layer diagonal and off-diagonal current-voltage relationships that can be used to identify this state experimentally.

DOI: 10.1103/PhysRevB.106.224504

I. INTRODUCTION

Superconductivity is a well-explored yet still puzzling phenomena of the collective behavior of electrons. The microscopic Bardeen–Cooper–Schrieffer (BCS) [1,2] theory explains it in terms of bound (Cooper) electron pairs due to effective attractive interactions. The condensation of Cooper pairs gives rise to a non-Fermi-liquid state with spontaneously broken $U(1)$ symmetry characterized by a homogenous complex order parameter Δ. One signature of superconductivity is a nonlinear junction resistance with a normal metal. At subgap values of the bias voltage on the interface, the only way for a single electron to penetrate inside a superconductor is to form a Cooper pair. Therefore, by charge conservation, transmission through the interface should be accompanied by reflection of a hole, a process known as Andreev [3] reflection. Studies of Andreev reflection can be used to probe [4,5] a state of interest and continue to gather both theoretical [6–13] and experimental [14–17] attention.

In recent years experimentalists uncovered examples of both electron-electron (Cooper) and electron-hole (excitonic) pairing in atomically thin two-dimensional materials[18–23]. In general, Cooper pairing is driven by attractive effective interactions and electron-hole pair formation by repulsive interactions between electrons in different bands. Exciton condensates [24–29] are coherent states of electrons and holes bound into pairs by the Coulomb interaction and are described by a mean-field theory that is identical to BCS theory apart from a particle-hole transformation. In bulk materials the concept of exciton condensation is partly ambiguous since the ordered states are difficult to distinguish from density-wave or nematic states [30]. Although exciton condensates were predicted theoretically more than 50 years ago, their experimental identification in bulk materials has suffered as a consequence, although progress was achieved recently [31–33]. Experimental advances with two-dimensional materials solved the ambiguity problem by making it possible to prepare devices with strong interactions between subsystems located in different layers that separately have nearly perfectly conserved particle number. Interlayer coherence is a related yet slightly different phenomena. It corresponds to the same order parameter and also breaks the independent gauge invariance of the individual layers: i.e., when the exciton order parameter x is nonzero we no longer can perform gauge transformation in two layers independently. However, interlayer coherence, unlike the exciton condensation, does not open a gap in the system and bears more similarity to pseudospin magnetism. There are still only a few examples of convincing experimental evidence for the excitonic condensation and interlayer coherence in systems without a strong external magnetic field, but this situation seems likely to change.

Recently, superconductivity was observed in magic angle twisted bilayer graphene (tBG) [34,35], a two-dimensional system with a moiré superlattice that yields extremely flat conduction and valence bands. The strongest superconductivity appears when the valence band is doped away from half filling. Although several models [36–40] for its superconductivity have been proposed, the mechanism remains unknown. Twisted bilayers are the simplest examples of a rich variety of graphene multilayer moiré superlattice systems that have received experimental attention recently [41–45]. The motivation for this paper is to consider the possibility of realizing, in this flexible family of strongly correlated electron systems, an exotic state in which interlayer coherence and superconductivity occur simultaneously. Our target system is two twisted bilayers separated by a hexagonal boron nitride tunnel barrier. The superconductivity of the individual twisted bilayers is already established. Here we ask the following questions: (i) can interlayer coherence occur, in principle, between

[*]blinov@utexas.edu

2469-9950/2022/106(22)/224504(11)

two-dimensional electron systems that are superconducting and (ii) if so, how would such a state be most unambiguously detected? So far research on the coexistence of two phases, or, broadly speaking, multicomponent coupled condensates, has been scarce [46–48] partially because of the lack of a physical system with a potential to have both. In this paper, we study the possibility for a system to have both interlayer coherence (magnetism in layer-pseudospin label) and superconductivity within each layer: a state in which two superconducting states within each layer are coupled through the spontaneously established interlayer coherence. In Sec. II we describe the model and study the relationships between its order parameters. In Sec. III we describe the phases we identified and phase diagrams as a function of the strength of the interlayer repulsive interaction strength g_x and the intralayer attractive interaction strength g_s. In Sec. IV we propose an Andreev drag measurement which can be used to identify states with both types of order, taking advantage [49] of the possibility of separate contacting to individual layers. This method of probing bilayer exciton condensates was very successfully exploited in quantum Hall excitonic superfluids [50–54] Finally, in Sec. V, we discuss prospects for observing these states and the importance of deviations from the highly symmetric point that we considered in our explicit calculations.

II. MODEL

We consider the simplest possible model that can have both interlayer coherence and s-wave superconductivity. The model assumes that both the attractive intralayer and repulsive interlayer interactions are momentum independent, includes a layer degree of freedom ($l = t, b$), and assumes either valley or spin singlet superconductivity. The Hamiltonian

$$H = \sum_{pl\sigma} \xi_{pl} c^{\dagger}_{l\sigma}(p) c_{l\sigma}(p) + \frac{\lambda_s}{S} \sum_{pp'q} c^{\dagger}_{l\uparrow}(p+q) c^{\dagger}_{l\downarrow}(p'-q) c_{l\downarrow}(p') c_{l\uparrow}(p) + \frac{\lambda_x}{S} \sum_{pp'q} c^{\dagger}_{t\sigma}(p+q) c^{\dagger}_{b\sigma'}(p'-q) c_{b\sigma'}(p') c_{t\sigma}(p), \quad (1)$$

where $c^{\dagger}_{l\sigma}$ ($c_{l\sigma}$) creates (annihilates) a fermion in layer $l = t, b$ with pseudospin $\sigma =\uparrow, \downarrow$, and S is the area of the sample, $\xi_{pl\sigma} = \epsilon(p)_{l\sigma} - \mu_l$ where $\epsilon(p)_{l\sigma}$ is a dispersion relation and μ_l is the Fermi energy within the layer. In this work, we will focus on the case of layer-independent bands, $\xi_{pl} \equiv \xi_p$ (Fig. 1), and reserve discussion of the deviations from this symmetric limit to the end of the paper. (As we explain in Sec. V coexistence does not occur for $\xi_{pt} \equiv -\xi_{pb}$.) The pseudospin label refers to the real spin in the case of spin-singlet superconductors and to the valley in the case of valley-singlet superconductors. Below we refer to this degree of freedom as spin for simplicity. Below we characterize the ordered states by their mean-field Hamiltonians and allow an exciton order parameter for each spin species

$$x_\sigma = \frac{\lambda_x}{S} \sum_p \langle c_{t\sigma}(p) c^{\dagger}_{b\sigma}(p) \rangle, \quad (2)$$

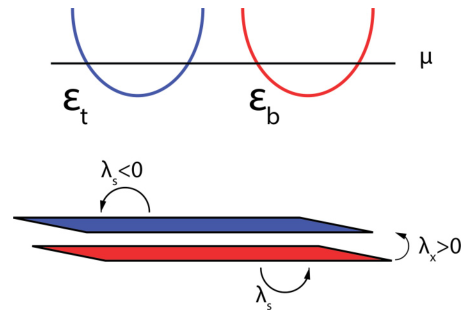

FIG. 1. Sketch of the band alignment and the configuration of the layers. We take energy dispersion to be the same in both layers as well as the electron filling. Interactions within the layer ($\lambda_s < 0$) are attractive while between the layers ($\lambda_x > 0$) is repulsive. We talk about deviations from the perfectly symmetric scenario in the discussion section.

and superconducting order parameters both within and between layers

$$\Delta^{ll'}_{\sigma\sigma'} = -\frac{\lambda_{ll'}}{S} \sum_p \langle c_{l\sigma}(p) c_{l'\sigma'}(-p) \rangle, \quad (3)$$

where $\lambda_{tt} = \lambda_{bb} = \lambda_s$ and $\lambda_{tb} = \lambda_{bt} = \lambda_x$. The ordered state is therefore characterized by six complex self-energies that vanish if no symmetries are broken.

In single-band superconductors, the pair potential can be chosen to be real because of global gauge invariance. It follows that one real number, the gap, fully characterizes the superconducting phase. In the present two-band system, we start with four complex pair potentials. If we also allow excitonic particle-hole pairing for both spins, the ordered state is characterized by 12 real numbers. Since only three phases can be chosen at will by exploiting the conservation of the number of particles of particles of each spin in each layer, the energy can depend not only on absolute values of the order parameters, but also on their phases, or, more specifically, on gauge-invariant combinations of such phases.

In the absence of interlayer superconducting coupling, there is only one gauge-invariant combination of the phases $\psi_t - \psi_b - \psi_\uparrow - \psi_\downarrow$, where $\psi_{\sigma=\uparrow,\downarrow}$ is the phase of the corresponding exciton pair potential and $\psi_{l=t,b}$ is the phase of the intralayer superconducting pairing potential. This combination changes sign under layer flip. If we assume that the ground state preserves spin and layer invariance, we see that

$$\psi_t - \psi_b - \psi_\uparrow - \psi_\downarrow = \pi n, \quad (4)$$

where n is an integer. In the gauge $\psi_b = 0$, $\psi_\uparrow = 0$, $\psi_\downarrow = 0$, an even n will correspond to a state with two superconducting gaps having the same sign, while an odd n will correspond to a state with superconducting gap that changes sign under the layer flip.

To extend this analysis to the case with nonzero interlayer pairing, we identify four gauge-invariant quantities that do not transform to themselves under layer or spin inversion: $x_\uparrow \Delta^{bt}_{\uparrow\downarrow} \Delta^{tt}_{\uparrow\downarrow}{}^*$, $x_\downarrow \Delta^{bt}_{\downarrow\uparrow} \Delta^{tt}_{\downarrow\uparrow}{}^*$, $x^*_\uparrow \Delta^{tb}_{\uparrow\downarrow} \Delta^{bb}_{\uparrow\downarrow}{}^*$, and $x^*_\downarrow \Delta^{tb}_{\downarrow\uparrow} \Delta^{bb}_{\downarrow\uparrow}{}^*$ and require that their values do not change under these transformations [55]. This condition restricts the absolute values of all self-energies $|\Delta^t| = |\Delta^b| \equiv \Delta_d$, $|x_\uparrow| = |x_\downarrow| \equiv x$, $|\Delta^{tb}_{\uparrow\downarrow}| =$

$|\Delta^{bt}_{\uparrow\downarrow}| \equiv \Delta_i$ as well as two gauge-invariant combinations of phases

$$\psi_1 - \psi_2 = \psi_\downarrow - \psi_\uparrow - 2\pi m, \tag{5}$$

$$\psi_t - \psi_b = \psi_\uparrow + \psi_\downarrow - 2\pi k, \tag{6}$$

where ψ_1 is the phase of $\Delta^{bt}_{\uparrow\downarrow}$ and ψ_2 is the phase of $\Delta^{tb}_{\uparrow\downarrow}$, k and m are integers. (d, and i in Δ_d and Δ_i are intended to suggest *direct* and *indirect* pairing.)

The system has one more independent gauge-invariant combination of phases $\psi_t + \psi_b - \psi_1 - \psi_2 \equiv 2\psi_+$. Unlike those we considered previously, this combination transforms to itself under layer or spin flip, and therefore should be determined by energy minimization.

Using global gauge invariance related to conserved particle numbers for each spin and valley ψ_1, $\psi_\uparrow$, and $\psi_\downarrow$ can be chosen to be 0. Then because of (5) $\psi_2 = 2\pi m$ and $\psi_- \equiv (\psi_t - \psi_b)/2 = \pi k$. In what follows, we use this gauge. This leaves us with mean-field Hamiltonians that depend only on four parameters. There are three absolute values: Δ_d (direct superconducting gap, particle-particle pairing within a layer), Δ_i (indirect superconducting gap, particle-particle pairing between the layers), x (electron-hole coherence between the two layers), and a single free phase [$\psi_+ \equiv (\psi_t + \psi_b)/2$], whose values can be determined by solving self-consistent field equations.

III. PHASE DIAGRAM

We saw previously that layer and spin symmetries restrict the value of ψ_-, but not $\psi_+ \equiv (\psi_t + \psi_b)/2$. In this section, we allow both phases to take any value to demonstrate explicitly that energies are minimized when spin/layer symmetries are respected: the four distinct allowed values of ψ_- (0, $\pi/2$, $3\pi/2$ π if $\Delta_i = 0$ and 0 π if $\Delta_i \neq 0$) follow from the self-consistency equations. The mean-field version of (1) can be written as

$$H_{mf} = \sum_p \Psi^\dagger(p)\mathcal{H}(p)\Psi(p), \tag{7}$$

where $\Psi^\dagger(p) = (c^\dagger_{t\uparrow}, c_{t\downarrow}, c^\dagger_{b\uparrow}, c_{b\downarrow})$ is a vector in an extended Nambu space and the Hamiltonian matrix is

$$\mathcal{H}(p) = \begin{pmatrix} \xi_p & \Delta_d e^{i(\psi_+ + \psi_-)} & x & \Delta_i \\ \Delta_d e^{-i(\psi_+ + \psi_-)} & -\xi_p & \Delta_i & -x \\ x & \Delta_i & \xi_p & \Delta_d e^{i(\psi_+ - \psi_-)} \\ \Delta_i & -x & \Delta_d e^{-i(\psi_+ - \psi_-)} & -\xi_p \end{pmatrix}. \tag{8}$$

The negative eigenvalues of the matrix have the form $\epsilon_\pm = -(\eta^2 \pm 2\alpha^2)^{1/2}$, where $\eta^2 = \xi^2 + x^2 + \Delta_i^2 + \Delta_d^2$ and $\alpha^4 = x^2\Delta_d^2 \sin^2(\psi_-) + 2\Delta_d\Delta_i x\xi \cos(\psi_+)\cos(\psi_-) + \Delta_i^2\Delta_d^2\cos^2(\psi_+) + (x\xi)^2$. Stable phases of the system are determined by minimization of the energy density. At energy extrema

$$E = \frac{2\Delta_d^2}{|\lambda_s|} - \frac{2\Delta_i^2}{\lambda_x} + \frac{2x^2}{\lambda_x} + \sum_b \int d\xi\, \nu(\xi)\epsilon_b n_b(\xi), \tag{9}$$

where the sum is over quasiparticle bands b, $\nu(\xi)$ is the quasiparticle density of states per spin and per layer, and $n_b(\xi)$ is the Fermi occupation factor. At zero temperature, only quasiparticle states with negative energies are filled.

The extrema of the energy are also extrema of (9), which we vary first with respect to the phases ψ_- and ψ_+. We conclude that energy minima occur at the extrema of α^2 and that these occur (independent of ξ_p) when

$$\sin(\psi_+) = 0 \text{ and } \sin(\psi_-) = 0, \tag{10}$$

or

$$\cos(\psi_+) = 0 \text{ and } \cos(\psi_-) = 0. \tag{11}$$

The first condition is consistent with the conditions we derived for a mirror- and spin-symmetric state with $\Delta_i \neq 0$. We will call it a parallel phase. The second condition defines the antiparallel phase [56]. We will see that the second conditin is consistent only with $\Delta_i = 0$. Note that each condition, in fact, corresponds to two different states. Namely, (10) can be satisfied with $(\psi_t, \psi_b) = (\pi, \pi)$, and (0,0), that typically have different energies when interlayer superconducting order is present. Now we consider the antiparallel and parallel phases separately.

A. Antiparallel phase

We consider first the extrema in which the phases ψ_t and ψ_b differ by π. The main conclusion of this subsection is that, for any sufficiently smooth density of states, the energy of the antiparallel phase is always higher than that of a pure superconducting phase. In other words, this solution of the mean-field equations corresponds to a local energy maximum not an energy minimum, and can therefore be discarded. In the antiparallel phase, variation of the energy density in (9) with respect to Δ_i combines with (11) to yield the self-consistency equation

$$\Delta_i = -\frac{\lambda_x\Delta_i}{4}\int \nu(\xi)\left(\frac{1}{\epsilon_+} + \frac{1}{\epsilon_-}\right). \tag{12}$$

This equation clearly cannot be satisfied at any $\lambda_x > 0$. We conclude that $\Delta_i = 0$ in the antiparallel phase. The quasiparticle band energies are therefore

$$\pm\epsilon_\pm = \pm\left|\sqrt{\xi^2 + \Delta_d^2} \pm x\right|. \tag{13}$$

The form of the band energies allows us to identify the antiparallel phase as an exciton condensate (spontaneous interlayer phase coherent state) formed on top of superconductors within each of the layers. With Δ_i eliminated, the system of gap equations reduces to

$$x = \lambda_x \mathcal{N}\left(\sqrt{x^2 - \Delta_d^2}\right), \tag{14}$$

$$\Delta_d = -\frac{\lambda_s \Delta_d}{2} \int \frac{\nu(\xi)}{\sqrt{\xi^2 + \Delta_d^2}} + \frac{\lambda_s \Delta_d}{2} \int_{-\sqrt{x^2-\Delta_d^2}}^{\sqrt{x^2-\Delta_d^2}} \frac{\nu(\xi)}{\sqrt{\xi^2 + \Delta_d^2}}. \tag{15}$$

That is to say that the exchange self-energy is contributed by wave vectors that have different occupation numbers for the two orthogonal quasiparticle layer spinors. In (14) $\mathcal{N}(\epsilon) \equiv 1/2 \int_{-\epsilon}^{\epsilon} d\xi \; \nu(\xi)$.

A transition between pure superconductivity and an antiparallel phase would occur at zero temperature if the later phase were lower in energy. We find that

$$\begin{aligned} E_m - E_{\rm sc} = {} & \frac{2}{|\lambda_s|}\left(\Delta_{d\,m}^2 - \Delta_{d\,0}^2\right) \\ & - 2\int_{-\mu}^{\Lambda} \nu(\xi)\left(\sqrt{\xi^2 + \Delta_{d\,m}^2} - \sqrt{\xi^2 + \Delta_{d\,0}^2}\right) \\ & + 2\int_{-\sqrt{x^2-\Delta_{d\,m}^2}}^{\sqrt{x^2-\Delta_{d\,m}^2}} \nu(\xi)\sqrt{\xi^2 + \Delta_{d\,m}^2} \\ & - 2x\mathcal{N}\left(\sqrt{x^2 - \Delta_{d\,m}^2}\right) \leqslant 0, \end{aligned} \tag{16}$$

where we distinguish the superconducting gap $\Delta_{d\,m}$ in the mixed phase from the superconducting gap Δ_{d0} in the pure superconducting phase and used a self-consistency equation to reexpress the last term. Since the energy of the pure superconducting phase is minimized by Δ_{d0}, we can conclude that the sum of the first two lines in (16) is nonnegative. Provided that the density of states does not significantly vary on the scale of $\sqrt{x^2 - \Delta_{d\,m}^2}$, the third line can be approximated by

$$2\nu_0 \Delta_{d\,m}^2 \sinh^{-1}\left(\frac{\sqrt{x^2 - \Delta_{d\,m}^2}}{\Delta_{d\,m}}\right), \tag{17}$$

where ν_0 is the constant density of states and the full energy difference is positive. Hence, at least for a sufficiently smooth density of states, the antiparallel phase will never be thermodynamically stable. We now analyze the parallel phase.

B. Parallel phase

The parallel phase is defined by the conditions $\sin(\psi_+) = 0$, $\sin(\psi_-) = 0$, so that ψ_t and ψ_b are equal to within a multiple of 2π. This condition, however, leaves an ambiguity since the $\cos(\psi_+)\cos(\psi_-)$ factor present in the dispersion relation can be either $+1$ or -1. We distinguish these possibilities by introducing $f = 0, 1$ such that $\cos(\psi_+)\cos(\psi_-) = (-1)^f$. The quasiparticle energies can be expressed as

$$\epsilon_\pm = \sqrt{(\xi \pm x)^2 + [\Delta_d \pm (-1)^f \Delta_i]^2}. \tag{18}$$

We can interpret this phase as two superconductors: one with Cooper pairs formed out of symmetric combinations of layers, another from antisymmetric combinations. Indeed, the mean-field Hamiltonian matrix (7) is block-diagonal in this basis. Note here that even though the transformation to the symmetric and antisymmetric states block-diagonalizes $\mathcal{H}(p)$, energy density E (9) will still have terms that couple the two unless $|\lambda_s| = \lambda_x$. Solutions with $f = 0/1$ then correspond to phases within which either symmetric or antisymmetric superconducting gaps are larger. Variation of the full energy density (9) with respect to Δ_i yields

$$\begin{aligned} \frac{\delta E}{\delta \Delta_i} = {} & -\frac{4\Delta_i}{\lambda_x} - \Delta_i \int \nu(\xi)\left(\frac{1}{\epsilon_-} + \frac{1}{\epsilon_+}\right) \\ & + (-1)^f \Delta_d \int \nu(\xi)\left(\frac{1}{\epsilon_-} - \frac{1}{\epsilon_+}\right). \end{aligned} \tag{19}$$

We see here that the $\Delta_i = 0$ point is not an energy extremum whenever both exciton condensates and superconductivity are present. Note that the superconducting gap of the symmetric quasiparticles is $\Delta_d + (-)^f \Delta_i$, while for the antisymmetric quasiparticles is $\Delta_d - (-)^f \Delta_i$. Because the exciton condensate breaks the symmetry between quasiparticle bands, one should expect that $\Delta_d + \Delta_i \neq \Delta_d - \Delta_i$. A complimentary explanation is that, even though the interlayer interaction is repulsive, the BCS instability present within each layer together with interlayer coherence induces a response in the interlayer Cooper channel: Δ_i is induced by the coexistence of the exciton condensate and superconductivity. It would not acquire nonzero value in the isolation.

If we write the self-consistency equations in terms of $\Delta_- \equiv \Delta_d - (-1)^f \Delta_i$, $\Delta_+ \equiv \Delta_d + (-1)^f \Delta_i$ and x we obtain

$$\frac{1}{\lambda_-^2 - \lambda_+^2}(\lambda_+\Delta_+ - \lambda_-\Delta_-) = \frac{\Delta_+}{2} \int \frac{d\xi\,\nu(\xi)}{\sqrt{(\xi + x)^2 + \Delta_+^2}}, \tag{20}$$

$$\frac{1}{\lambda_-^2 - \lambda_+^2}(\lambda_+\Delta_- - \lambda_-\Delta_+) = \frac{\Delta_-}{2} \int \frac{d\xi\,\nu(\xi)}{\sqrt{(\xi - x)^2 + \Delta_-^2}}, \tag{21}$$

$$\frac{4}{\lambda_+ - \lambda_-} x = \int \frac{d\xi\,\nu(\xi)(x - \xi)}{\sqrt{(\xi - x)^2 + \Delta_-^2}} + \int \frac{d\xi\,\nu(\xi)(x + \xi)}{\sqrt{(\xi + x)^2 + \Delta_+^2}}. \tag{22}$$

Here $\lambda_+ \equiv (\lambda_s + \lambda_x)/2$ and $\lambda_- \equiv (\lambda_s - \lambda_x)/2$. Note that, even though the mean-field Hamiltonian matrix is block diagonal in the basis of the symmetric and antisymmetric combinations of two layers, the energy density has a term of the form $\Delta_+\Delta_-$ because $\lambda_s \neq \lambda_x$. The mixed-state solution summarized in Fig. 2 exists for $\nu(0)\lambda_x \geqslant 1$. In the numerical calculation, to treat both $f = 0$ and $f = 1$ minima on equal footing, we allowed the interlayer superconducting gap Δ_i to take negative values. This extension does not have any physical significance, as the discreteness of f comes from the energy minimization. Negative value of Δ_i corresponds to the $f = 1$ minimum while positive values will correspond to the $f = 0$ minimum. Our calculation shows that the $f = 1$ minimum tend to be more energetically favorable for larger values of intralayer attraction, which has a simple physical meaning: for $|\lambda_s| \approx \lambda_x$ the symmetric and the antisymmetric superconductors are effectively decoupled and thus the larger gap corresponds to a larger effective Fermi energy $\mu \pm x$ (see Appendix B). Along the first-order phase boundary in g_s/g_x

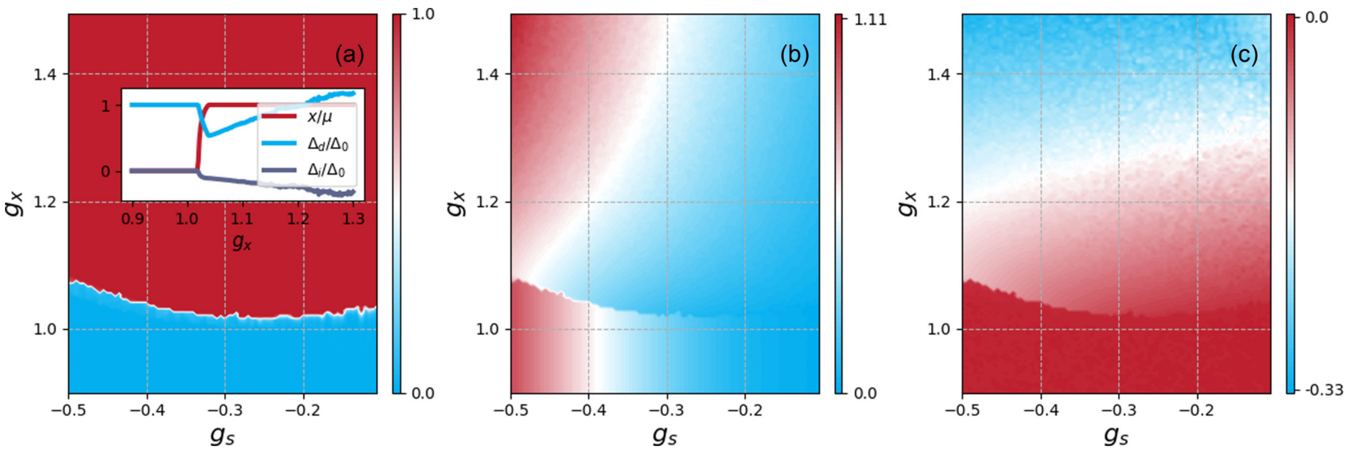

FIG. 2. Order-parameter dependence on dimensionless interaction constants $g_s = \nu\lambda_s$ and $g_x = \nu\lambda_x$ in the parallel phase, where ν is the parabolic band density of states. The normalized exciton self-energy x/μ is plotted in (a), where μ is the Fermi energy. At small $|g_s|$ there is a phase transition at $g_x = 1$, which is first order in our model, to a large g_x state with $x \neq 0$. The normalized intralayer superconducting self-energy Δ_d/Δ_0, where Δ_0 its maximal value in the pure superconducting phase, plotted in (b) is always nonzero. The normalized interlayer superconducting self-energy Δ_i/Δ_0 is plotted in (c) and acquires a finite value only when $x \neq 0$. At the transition the purely intralayer superconducting phase to the mixed phase, Δ_d (b) decreases. For large values of $|g_s|$ the excitonic transition is pushed to larger values of g_x. The inset in (a) shows the three self-energies as a function of g_x at a fixed $g_s = -0.4$. These results were obtained for cutoff $\Lambda = 10$ meV, $\epsilon_F = 3$ meV, and a parabolic band model with a constant density of states. To treat both $f = 0$ and $f = 1$ minima on the equal footing, we allow the interlayer superconducting gap Δ_i to take negative values. Self-energies are in units of meV. We minimized energy as a function of the Bogolyubov angles using the conjugate graduate method.

space separating mixed and pure superconducting phases, the two states have identical energies. It follows that the differential energy changes $dE_{\rm sc}$ in the superconducting phase and $dE_{\rm mix}$ in the mixed phase should be the same. It follows that the slope of the phase boundary lines

$$\frac{dg_x}{dg_s} = \frac{\frac{\partial E_{\rm sc}}{\partial g_s} - \frac{\partial E_{\rm mix}}{\partial g_s}}{\frac{\partial E_{\rm mix}}{\partial g_x}}. \tag{23}$$

Partial derivatives in the formula will be proportional to order parameters in each phase: $\partial E_{\rm sc,mix}/\partial g_s = -2\Delta^2_{\rm sc,mix}/g_s^2$, $\partial E_{sc}/\partial g_x = 2(x^2 - \Delta_i{}^2)/g_x^2 \approx 2\mu^2/g_x^2$. Formation of the mixed state accompanied by the immediate decrease in the superconducting gap at least for large enough $|g_s|$. Therefore, $dg_x/dg_s < 0$ — for larger attractive interaction the g_s transition will happen at a larger critical g_x in agreement with Fig. 2. Physically, it corresponds to the fact that the mixed parallel and purely superconducting phases are competing. Because with larger attraction within the layer it is more energetically beneficial to have larger superconducting gaps, the purely superconducting phase could be more energetically favorable and thus the boundary between the phases goes up. Further increase in the interlayer repulsion leads to the enhancement of the superconductivity. It is easier to see, however, that in the limit of infinite repulsion $\lambda_x \gg |\lambda_s|$ between layers the gap equations (20) and (21) are again governed by the the intralayer attraction λ_s.

IV. NONLOCAL ANDREEV REFLECTION

Having established that an exotic mixed state with both excitonic and Cooper pair order can exist, we now discuss Andreev reflection experiments in separately contacted bilayers that can be used to detect their presence. Consider metallic leads separately connected to the top and the bottom layers of our system. An electron incident on the interface between the top lead and the top layer has equal weight in symmetric and antisymmetric quasiparticle channels $|t\rangle = (|+\rangle + |-\rangle)2^{-1/2}$. Since the parallel state does not couple $|+\rangle$ with $|-\rangle$, we can consider their transmission contributions separately, at least if disorder is neglected. Incoming from the top quasiparticles are reflected with probabilities A_{tt} (tt stands for top → top) and A_{tb} (tb stands for top → bottom) as holes, and with probabilities B_{tt} and B_{tb} as electrons, to the top and bottom layers, respectively. The respective amplitudes are denoted with small letters (a_{tt}, a_{tb}, b_{tt}, b_{tb}). The calculation of these reflection amplitudes is discussed below.

If we apply V for voltage across the top part of the interface, the top and bottom layer differential conductances will be connected to reflection coefficients in a normal fashion. The total currents in the top and bottom layers are

$$I_{t/b} = e\nu_0 \int_0^{eV} d\omega\, \sigma_{t/b}(V), \tag{24}$$

where

$$\sigma_t(V) \equiv dj_t/dV = e^2 v_f \nu_0 [1 - B_{tt}(V) + A_{tt}(V)],$$
$$\sigma_b(V) \equiv dj_b/dV = e^2 v_f \nu_0 [A_{tb}(V) - B_{bt}(V)], \tag{25}$$

e is an electron charge, and $v_f \nu_0$ is the product of the Fermi velocity and the density of states. Note that the combination $A_{tb} - B_{tb}$ (A_{tb} is a probability to reflect an incoming from the top electron as hole to the bottom layer, B_{tb} is a probability to reflect it as an electron) of cross-layer reflection probabilities can be measured experimentally. We derive expressions for the scatterring amplitudes in the Appendix using the Bogoliubov–de Gennes equations. The amplitude to reflect an electron as a hole in either symmetric or antisymmetric states, at least in the limit $x \ll \mu$, around 1 at $\omega = 0$ similarly to a single N-S junction. However, the amplitude to reflect an incoming electron as an electron is no longer negligible even in the $\Delta_d \ll \mu$ case. The electron reflection amplitude at $\omega = 0$ is given by $b_\pm \approx \mp x/(2\,\mu \pm x)$. Because b_+ and b_- have opposite signs, the probability to reflect an electron to the bottom layer $B_{tb} = |b_+ - b_-|^2/4$ is substantially higher than the probability of the corresponding Andreev process, which is almost zero. For the the same reason electron reflection in the top layer is unimportant for small ω and instead the Andreev process dominates (Fig. 3). When energy is equal to the + or − gap and the gap $\Delta_\pm/\mu \ll 1$, the corresponding momenta in the leads and device match, giving rise to peaks in Andreev reflection and minima in electron reflection. As a result the Andreev process is stronger than the electron reflection in the bottom layer. Altogether, we expect $A_{tb} - B_{tb}$ to have a μ-like shape, with negative values around $\omega = 0$ and positive peaks at the superconducting gaps (Fig. 3).

If we follow the standard practice [57] of modeling interface disorder by a delta-function potentials $v_l\delta(z)$, $\langle v\rangle = (v_t + v_b)/2$ will play a role identical to that of the disorder in a regular superconductor by damping Andreev reflection at subgap energies and increasing electron-electron reflection in both symmetric and antisymetric channels. The dimensionless quantity controlling its importance is $\langle v\rangle/v_F$, where v_F is the Fermi velocity. Any difference $\Delta v = (v_t - v_b)/2$ between layers in the disorder parameter values will couple the symmetric and antisymmetric quasiparticle channels. The importance of these corrections is, however, also controlled by $\Delta_d v/v_F$, and for values $\Delta_d v/v_F < 0.5$ there is no qualitative change in the μ-like shape of the differential conductance (Fig. 4). Sufficiently large values of $\Delta_d v/v_F$ raise the low-energy part of the differential conductance to positive values.

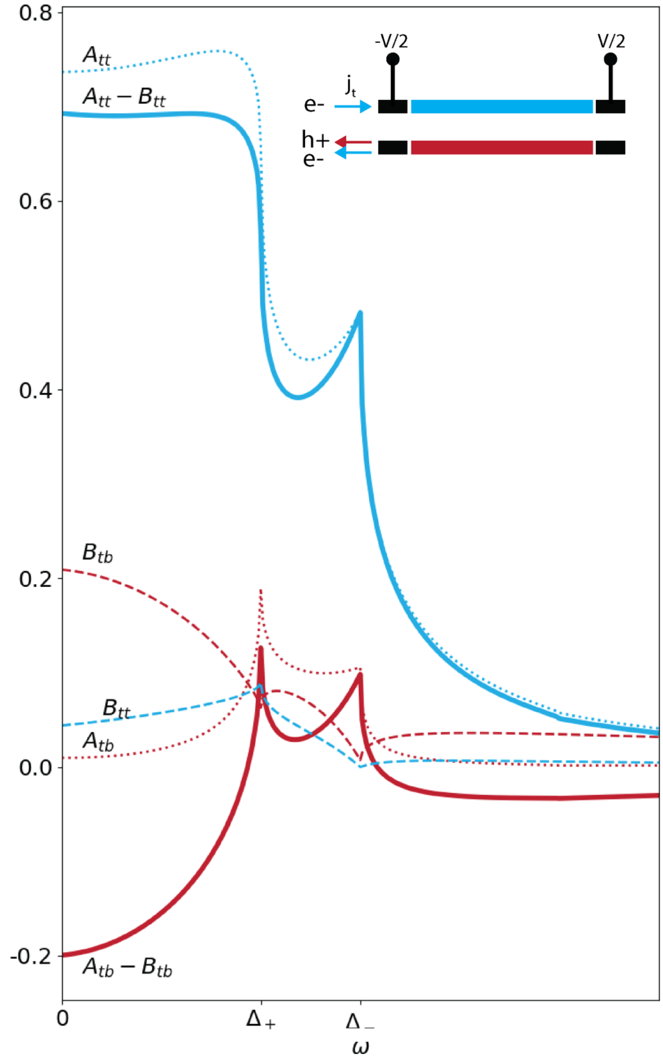

FIG. 3. Probabilities for an electron coming from the top lead at energy ω to be reflected as a hole/electron in the same layer (A_{tt}/B_{tt}), and as a hole/electron in the opposite layer (A_{tb}/B_{tb}). The quantity $A_{tb} - B_{tb}$, proportional to the differential conductance in the bottom layer, changes sign as function of ω. At low energies, the conductance is dominated by electron-electron reflection. At energies around superconducting gaps, the conductance is dominated by Andreev reflection processes. The inset shows a schematic experimental device with voltage bias V across the top layer. When mesoscopic effects are neglected, the top layer conductance of the device is $\sigma_t(V/2)/2$, where $\sigma_t(V)$ is the differential conductance between the top left lead and the top layer, and the transconductance driven by excitonic order is $\sigma_b(V/2)/2$, where $\sigma_b(V)$ is the conductance between the top left lead and the bottom layer.

V. DISCUSSION

In recent years experimenters established moiré heterojunctions as attractive platforms [58] for new types of two-dimensional electron ground states. In this article, we explored the phase diagram of bilayers with attractive effective interactions (λ_s) within each layer and repulsive interactions (λ_x) between layers. Two-dimensional bilayers with repulsive interlayer interactions can [21] have excitonic insulator ground states that are counterflow superfluids and have spontaneous interlayer phase coherence. Our work is motivated by the discovery of superconductivity, and hence attractive effective interactions, in graphene bilayers [35,43] and trilayers [44]. We therefore address the possibility of states that have both superconductivity and interlayer coherence, and study how the occurrence of such exotic states would be manifested by generalized Andreev effects in separately contacted bilayers.

With this goal we performed mean-field calculations for a model bilayer Hamiltonian with two identical layers and attractive intralayer and repulsive interlayer interactions. We neglected tunneling τ between the layers, assuming that the bilayers are separated by dielectric layers. We stress here that unlike in [46], we study a system with the ordering between layers alike the magnetism. The difference is that, unlike in the scenario with excitonic condensation, there is no gap established directly through the interlayer coherence.

Our calculations show that a mixed phase with both an interlayer exciton coherence and superconductivity appears over a wide range of model parameters. Interlayer coherence couples the two superconducting order parameters with energy extrema occurring when the pair amplitudes are in phase (parallel) and out of phase (antiparallel). We find that the energy of the antiparallel phase is higher than that of the pure

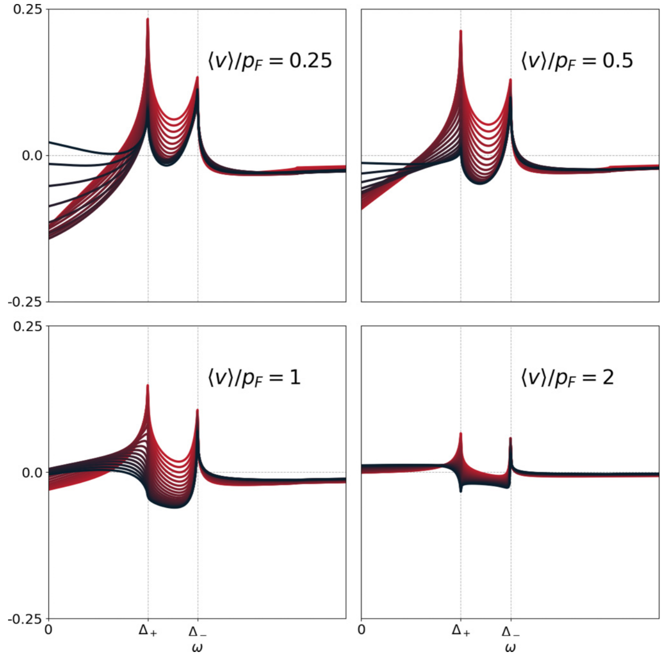

FIG. 4. Influence of interface disorder on the difference between hole (Andreev process) and electron interlayer reflection coefficients $A_{tb} - B_{tb}$. Disorder is modeled by a delta-function potential at the interface $v_I\delta(z)$. On each subplot, the ratio of $\langle v\rangle = (v_t + v_b)/2$ to the Fermi momentum is kept fixed. $\Delta v/p_F = (v_t - v_b)/(2p_F)$ is swept from -1.0 (red) to $+0.8$ (black) with step 0.1.

superconducting phase for any sufficiently smooth density of states. In the parallel phase superconducting state, interlayer coherence appears as a strong-coupling instability of states with superconductivity in each layer, and is established when $g_x \equiv \nu(\epsilon_F)\lambda_x > 1$. In twisted bilayer graphene we estimate that $\lambda_x \approx e^2/(4\pi k_F) \approx 100$ meVnm^2, and that the density of states is around $\nu(\xi_s) \approx 10^{-2}$ nm^{-2} meV^{-1} [59], implying that $g_x = 1$ is within reach. Since the superconducting transition temperature in tBG is $\sim$1 K, the value we chose for $|g_s| \lessapprox 1$ is not unrealistic. After interlayer coherence is established, further λ_x increases cause the superconducting order parameters to decay. Note that self-consistent solution with both exciton order parameter x and direct intralayer pairing Δ_d nonzero also have nonzero interlayer pairing Δ_i.

As a convenience, we limited our considerations to the case of two completely identical layers. This condition is, however, not important for the stability of the phase. Consider, for example, the case in which the Fermi energies in the two layers are slightly different: $\mu_{t,b} = \mu \pm \Delta\mu$. This change induces a perturbation to the mean-field Hamiltonian matrix of the form $-\tau_z\sigma^z\Delta\mu$, where τ^z and σ_z are the z-Pauli matrices acting on layer and Nambu indices correspondingly. After transformation to $+/-$ basis the perturbation acquire form $i\tau^y\sigma_z\mu$. As a result, there will be no first-order contribution to the quasiparticle energies. At second order, only matrix elements between positive and negative energy states will contribute. The leading-order correction to the quasiparticle energies will be small, $\sim(\Delta\mu^2/\sqrt{\Delta^2 + x^2})$. We conclude that small deviations from the perfect layer-symmetric case do not destroy the state, although they will change the mean-field-equation solutions quantitatively.

ACKNOWLEDGMENTS

We acknowledge support by the DOE Grant No. DE-FG02-02ER45958. I.V.B. thanks Nemin Wei, Ajesh Kumar, Rafi Bistritzer, and Pedro Ribeiro for interesting discussions.

APPENDIX A: BOGOLOYUBOV–DE GENNES EQUATION FOR THE PARALLEL STATE

Because Andreev reflection in symmetric and antisymmetric states cancel each other at zero voltage bias, it is instrumental to consider also electron-electron reflection. It is still true, however, that the Bogoliubov–de Gennes equation consists of two uncoupled systems of equations for a fully symmetric case. It is then sufficient to solve only one of them:

$$i\partial_t f = -\left(\frac{1}{2m}\frac{\partial^2}{\partial z^2} + \mu(z)\right)f + \Delta(z)\phi, \tag{A1}$$

$$i\partial_t \phi = \left(\frac{1}{2m}\frac{\partial^2}{\partial z^2} + \mu(z)\right)\phi + \Delta(z)f. \tag{A2}$$

The only difference from the classical [3,57] setup is that $\mu(z)$ is a function of a coordinate to take into account the presence of the interlayer coherence inside the system. Fourier transform with respect to the time $f(t) = \int e^{-i\omega t} f_\omega$ will give

$$\frac{1}{2m}\frac{\partial^2}{\partial z^2} f = -[\omega + \mu(z)]f + \Delta(z)\phi, \tag{A3}$$

$$\frac{1}{2m}\frac{\partial^2}{\partial z^2}\phi = [\omega - \mu(z)]\phi - \Delta(z)f, \tag{A4}$$

or, alternatively,

$$\frac{1}{2m}\frac{\partial^2}{\partial z^2}\begin{pmatrix} f \\ \phi \end{pmatrix} = \begin{pmatrix} -[\omega + \mu(z)] & \Delta(z) \\ -\Delta(z) & [\omega - \mu(z)] \end{pmatrix}\begin{pmatrix} f \\ \phi \end{pmatrix}. \tag{A5}$$

Let's assume that Δ changes abruptly from 0 to Δ_0 and similarly μ changes from μ to $\mu + x$:

$$\mu(z) = \mu + \theta(z)x, \tag{A6}$$

$$\Delta(z) = \theta(z)\Delta, \tag{A7}$$

where x can be both positive and negative. We solve it by writing it as a system of the first-order equations

$$\frac{1}{2m}\frac{\partial}{\partial z}\begin{pmatrix} f' \\ \phi' \\ f \\ \phi \end{pmatrix} = \begin{pmatrix} 0 & 0 & -(\omega + \mu) & \Delta \\ 0 & 0 & -\Delta & (\omega - \mu) \\ 1/2m & 0 & 0 & 0 \\ 0 & 1/2m & 0 & 0 \end{pmatrix}\begin{pmatrix} f' \\ \phi' \\ f \\ \phi \end{pmatrix}. \tag{A8}$$

Eigenvalues of this matrix are $\pm\frac{i}{\sqrt{2m}}(\mu + \sqrt{\omega^2 - \Delta^2})^{1/2}$, $\pm\frac{i}{\sqrt{2m}}(\mu - \sqrt{\omega^2 - \Delta^2})^{1/2}$. A general solution for $\omega < \Delta$ will be

$$\begin{pmatrix} f \\ \phi \end{pmatrix} = \frac{C}{\sqrt{2}} e^{iz\sqrt{2m}(\mu+i\sqrt{\Delta^2-\omega^2})^{1/2}} \begin{pmatrix} \sqrt{\frac{\omega+i\sqrt{\Delta^2-\omega^2}}{\Delta}} \\ \sqrt{\frac{\omega-i\sqrt{\Delta^2-\omega^2}}{\Delta}} \end{pmatrix} + \frac{D}{\sqrt{2}} e^{-iz\sqrt{2m}(\mu-i\sqrt{\Delta^2-\omega^2})^{1/2}} \begin{pmatrix} \sqrt{\frac{\omega-i\sqrt{\Delta^2-\omega^2}}{\Delta}} \\ \sqrt{\frac{\omega+i\sqrt{\Delta^2-\omega^2}}{\Delta}} \end{pmatrix}. \quad \text{(A9)}$$

We will denote in what follows $\sqrt{\frac{\omega+i\sqrt{\Delta^2-\omega^2}}{\Delta}} = u$ and $\sqrt{\frac{\omega-i\sqrt{\Delta^2-\omega^2}}{\Delta}} = v$ and $k_{sC} = \sqrt{2m}(\mu + i\sqrt{\Delta^2-\omega^2})^{1/2}$, $k_{sD} = \sqrt{2m}(\mu - i\sqrt{\Delta^2-\omega^2})^{1/2}$. On the left-hand side equations for a hole and an electron decouple and as a solution we get instead

$$\begin{pmatrix} f \\ \phi \end{pmatrix} = e^{i\sqrt{2m}z\sqrt{\omega+\mu_N}} \begin{pmatrix} 1 \\ 0 \end{pmatrix} + b e^{-i\sqrt{2m}z\sqrt{\omega+\mu_N}} \begin{pmatrix} 1 \\ 0 \end{pmatrix} + a \begin{pmatrix} 0 \\ 1 \end{pmatrix} e^{i\sqrt{2m}z\sqrt{\mu_N-\omega}}. \quad \text{(A10)}$$

The last piece is the reflected hole. Now boundary conditions read

$$1 + b = \frac{C}{\sqrt{2}}u + \frac{D}{\sqrt{2}}v, \quad \text{(A11)}$$

$$a = \frac{C}{\sqrt{2}}v + \frac{D}{\sqrt{2}}u, \quad \text{(A12)}$$

$$k_e(1-b) = \frac{C}{\sqrt{2}}uk_{sC} - \frac{Dk_{sD}}{\sqrt{2}}v, \quad \text{(A13)}$$

$$k_h a = \frac{C}{\sqrt{2}}vk_{sC} - \frac{Dk_{sD}}{\sqrt{2}}u, \quad \text{(A14)}$$

from which we conclude that

$$2 = \frac{Cu}{\sqrt{2}}\left(1 + \frac{k_{sC}}{k_e}\right) + \frac{Dv}{\sqrt{2}}\left(1 - \frac{k_{sD}}{k_e}\right), \quad \text{(A15)}$$

$$0 = \frac{Cv}{\sqrt{2}}\left(1 - \frac{k_{sC}}{k_h}\right) + \frac{Du}{\sqrt{2}}\left(1 + \frac{k_{sD}}{k_h}\right), \quad \text{(A16)}$$

hence

$$\frac{D}{C} = -\frac{v}{u}\frac{1 - \frac{k_{sC}}{k_h}}{1 + \frac{k_{sD}}{k_h}}, \quad \text{(A17)}$$

and so

$$2 = \frac{Cu}{\sqrt{2}}\left(1 + \frac{k_{sC}}{k_e}\right) - \frac{Cv^2}{u\sqrt{2}}\left(1 - \frac{k_{sD}}{k_e}\right)\frac{1 - \frac{k_{sC}}{k_h}}{1 + \frac{k_{sD}}{k_h}}, \quad \text{(A18)}$$

consequently,

$$C = \frac{2^{3/2}u\left(1 + \frac{k_{sD}}{k_h}\right)}{u^2\left(1 + \frac{k_{sC}}{k_e}\right)\left(1 + \frac{k_{sD}}{k_h}\right) - v^2\left(1 - \frac{k_{sD}}{k_e}\right)\left(1 - \frac{k_{sC}}{k_h}\right)}, \quad \text{(A19)}$$

$$D = -\frac{2^{3/2}v\left(1 - \frac{k_{sC}}{k_h}\right)}{u^2\left(1 + \frac{k_{sC}}{k_e}\right)\left(1 + \frac{k_{sD}}{k_h}\right) - v^2\left(1 - \frac{k_{sD}}{k_h}\right)\left(1 - \frac{k_{sC}}{k_h}\right)}. \quad \text{(A20)}$$

Expressions for amplitudes a and b are as follows:

$$a = \frac{2uv\left(\frac{k_{sD}}{k_h} + \frac{k_{sC}}{k_h}\right)}{u^2\left(1 + \frac{k_{sC}}{k_e}\right)\left(1 + \frac{k_{sD}}{k_h}\right) - v^2\left(1 - \frac{k_{sD}}{k_e}\right)\left(1 - \frac{k_{sC}}{k_h}\right)}, \quad \text{(A21)}$$

$$b = \frac{u^2\left(1 + \frac{k_{sD}}{k_h}\right)\left(1 - \frac{k_{sC}}{k_e}\right) - v^2\left(1 - \frac{k_{sC}}{k_h}\right)\left(1 + \frac{k_{sD}}{k_e}\right)}{u^2\left(1 + \frac{k_{sC}}{k_e}\right)\left(1 + \frac{k_{sC}}{k_h}\right) - v^2\left(1 - \frac{k_{sD}}{k_e}\right)\left(1 - \frac{k_{sC}}{k_h}\right)}. \quad \text{(A22)}$$

It is clear that a drastic change of the potential on the interface will lead to an increase in electron-electron scattering. Let us explore the low-energy properties of both a and b. Because at $\omega = 0$: $k_e = k_h = p_F$, where p_F is a Fermi momentum inside the metallic lead, $u = e^{i\pi/4}$, $v = e^{i3\pi/4}$. As a result, at $\omega = 0$,

$$a = -\frac{i\sqrt{\mu_N}(\sqrt{\mu - i\Delta} + \sqrt{\mu - i\Delta})}{\mu_N + \sqrt{\mu + i\Delta}\sqrt{\mu - i\Delta}}, \quad \text{(A23)}$$

$$b = \frac{(\sqrt{\mu_N} - \sqrt{i\Delta + \mu})(\sqrt{\mu_N} + \sqrt{\mu - i\Delta})}{\mu_N + \sqrt{\mu + i\Delta}\sqrt{\mu - i\Delta}}. \quad \text{(A24)}$$

Corresponding probabilities $A_{tt} = |a_+ + a_-|^2$, $A_{tb} = |a_+ - a_-|^2$, $B_{tt} = |b_+ + b-|^2$, $B_{tb} = |b_+ - b-|^2$. Because a for the symmetric and antisymmetric states are approximately equal to each other whenever $\mu \gg \Delta$, their difference is typically small if this condition is satisfied. Surprisingly, the electron-electron scattering amplitude does not vanish in the $\frac{\Delta}{\mu_N} \to 0$ limit because the effective Fermi energies inside and outside the system are different. When the ω is close to the gap, $u \approx v$, $k_C \approx k_D$, and if the gap is much smaller than μ_N, $k_e \approx k_h$, therefore, $b \approx 0$, $a \approx 1$. Thus, we expect the Andreev process to be dominant at frequencies corresponding to one of the gaps. If the disorder is present on the interface in the form $V_l(z) = v_l\delta(z)$, Bogoliubov–de Gennes equations are still decoupled in the bulk, but amplitudes are now coupled through the boundary conditions

$$1 + b_\pm = \frac{C_\pm}{\sqrt{2}}u_\pm + \frac{D_\pm}{\sqrt{2}}v_\pm, \quad \text{(A25)}$$

$$a_\pm = \frac{C_\pm}{\sqrt{2}}v_\pm + \frac{D_\pm}{\sqrt{2}}u_\pm, \quad \text{(A26)}$$

$$\begin{aligned}
&\frac{i}{2m}(u_\pm 2^{-1/2}C_\pm k_{\pm sC} - v_\pm 2^{-1/2}D_\pm k_{\pm sD} - k_e + k_e b_{+/-}) \\
&\quad = \langle v\rangle(C_\pm u_\pm 2^{-1/2} + D_\pm v_\pm 2^{-1/2}) \\
&\quad\quad - \Delta v(C_\mp u_\mp 2^{-1/2} + D_\mp v_\mp 2^{-1/2}) \\
&\frac{i}{2m}(v_\pm C_\pm 2^{-1/2}k_{\pm sC} - u_\pm D_\pm 2^{-1/2}k_{\pm sD} - k_h a_{+/-}) \\
&\quad = \langle v\rangle(C_\pm v_\pm 2^{-1/2} + D_\pm u_\pm 2^{-1/2}) \\
&\quad\quad - \Delta v(C_\mp v_\mp 2^{-1/2} + D_\mp u_\mp 2^{-1/2}),
\end{aligned}$$

where $\Delta v = (v_t - v_b)/2$, $\langle v\rangle = (v_t + v_b)/2$.

APPENDIX B: GREEN'S FUNCTION FORMALISM

In this Appendix we present equations of motion for zero-temperature Green's function and derive an important symmetry of self-energy in a way different from the one we took in the main text. In addition to a normal Green's function, we introduce a set of additional functions

$$iF^{l\dagger}_{\sigma\sigma'}(p,t_1-t_2)=\langle T(c^\dagger_{pl\sigma}(t_1)c^\dagger_{-pl\sigma'}(t_2))\rangle e^{-i2\mu_l t_1},\quad \text{(B1)}$$

$$iF^{l}_{\sigma\sigma'}(p,t_1-t_2)=\langle T[c_{pl\sigma}(t_1)c_{-pl\sigma'}(t_2)]\rangle e^{i2\mu_l t_1},\quad \text{(B2)}$$

$$iH^{tb}_{\sigma}(p,t_1-t_2)=\langle T(c_{pt\sigma}(t_1)c^\dagger_{pb\sigma}(t_2))\rangle e^{i(\mu_t-\mu_b)t_1},\quad \text{(B3)}$$

$$iD^{tb\dagger}_{\sigma\sigma'}(p,t_1-t_2)=\langle T(c^\dagger_{pt\sigma}(t_1)c^\dagger_{-pb\sigma'}(t_2))\rangle e^{-i(\mu_t+\mu_b)t_1},\quad \text{(B4)}$$

$$iD^{tb}_{\sigma\sigma'}(p,t_1-t_2)=\langle T[c_{pt\sigma}(t_1)c_{-pb\sigma'}(t_2)]\rangle e^{i(\mu_t+\mu_b)t_1}.\quad \text{(B5)}$$

Averages are taken over ground states with fixed and, in general, different number of particles of each kind. Because of this, averages are no longer dependent on the time difference. To mitigate this problem, averages are multiplied by an exponential with the difference between energies on the left and the right. I will only consider spatially uniform solutions and without spontaneous magnetization.

First, look at the equation of motion for the normal and the anomalous Green's functions

$$\left(i\frac{\partial}{\partial t}-\epsilon_{pt}\right)G_{t\uparrow}(p,t)=F^{t\dagger}_{\downarrow\uparrow}(p,t)\Delta^{tt}_{\uparrow\downarrow}+D^{bt\dagger}_{\downarrow\uparrow}(p,t)\Delta^{tb}_{\uparrow\downarrow}+H^{bt}_{\uparrow}(p,t)X^{tb}_{\uparrow}+\delta(t),\quad \text{(B6)}$$

$$\left(i\frac{\partial}{\partial t}+\epsilon_{pt}-2\mu_t\right)F^{t\dagger}_{\downarrow\uparrow}(p,t)=\bar{\Delta}^{tt}_{\uparrow\downarrow}G_{t\uparrow}(-p,t)+H^{bt}_{\uparrow}(-p,t)\bar{\Delta}^{bt}_{\uparrow\downarrow}-D^{bt\dagger}_{\downarrow\uparrow}(p,t)X^{bt}_{\downarrow},\quad \text{(B7)}$$

where we defined the self-energies

$$\Delta^{ll}_{\sigma\sigma'}=-\frac{i}{S}\sum V_{ll}(q)F^{l}_{\sigma\sigma'}(-p-q,0+),\quad \text{(B8)}$$

$$X^{ll'}_{\sigma}=\frac{i}{S}\sum V_{ll'}(q)H^{ll'}_{\sigma\sigma'}(p-q,0+),\quad \text{(B9)}$$

$$\Delta^{ll'}_{\sigma\sigma'}=-\frac{i}{S}\sum V_{ll'}(q)D^{ll'}_{\sigma\sigma'}(-p+q,0+),\quad \text{(B10)}$$

where $l\neq l'$, S is the area, and $V_{ll}(V_{ll'})$ is the intralayer (interlayer) interaction. Note here that positive V_{ll} means repulsion within the layer and similarly for $V_{ll'}$. The other two equations are

$$\left(i\frac{\partial}{\partial t}-\epsilon_{pb}-(\mu_t-\mu_b)\right)H^{bt}_{\uparrow}(p,t)=\Delta^{bb}_{\uparrow\downarrow}D^{\dagger bt}_{\downarrow\uparrow}(-p,t)+X^{bt}_{\uparrow}G^{t}_{\uparrow}(p,t)+\Delta^{bt}_{\uparrow\downarrow}F^{\dagger t}_{\downarrow\uparrow}(-p,t),\quad \text{(B11)}$$

$$\left(i\frac{\partial}{\partial t}+\epsilon_{pb}-(\mu_t+\mu_b)\right)D^{\dagger bt}_{\downarrow\uparrow}(p,t)=H^{bt}_{\uparrow}(p,t)\bar{\Delta}^{bb}_{\uparrow\downarrow}+G^{t}_{\downarrow}(-p,t)\bar{\Delta}^{tb}_{\uparrow\downarrow}-F^{\dagger t}_{\downarrow\uparrow}(p,t)X^{tb}_{\downarrow}.\quad \text{(B12)}$$

These equations can be either derived through equations of motion for operators or diagrammatically. Equations (B7) to (B12) constrain the form of the mean-field Hamiltonian. Indeed, consider a case without spin symmetry breaking $X^{tb}_{\uparrow}e^{-i\psi_\uparrow}=X^{tb}_{\downarrow}e^{-i\psi_\downarrow}$, $\Delta^{tt}_{\uparrow\downarrow}=-\Delta^{tt}_{\downarrow\uparrow}$, $G_\uparrow=G_\downarrow$. The last term means that each term in (B6) must be invariant under spin flip

$$H^{bt}_{\uparrow}e^{i\psi_\uparrow}=H^{bt}_{\downarrow}e^{i\psi_\downarrow},\quad \text{(B13)}$$

$$D^{bt\dagger}_{\downarrow\uparrow}(p,t)\Delta^{tb}_{\uparrow\downarrow}=D^{bt\dagger}_{\uparrow\downarrow}(p,t)\Delta^{tb}_{\downarrow\uparrow},\quad \text{(B14)}$$

$$F^{t\dagger}_{\downarrow\uparrow}(p,t)=-F^{t\dagger}_{\uparrow\downarrow}(p,t).\quad \text{(B15)}$$

From (B7) it follows then that

$$\frac{\bar{\Delta}^{bt}_{\uparrow\downarrow}}{\bar{\Delta}^{bt}_{\downarrow\uparrow}}=-\frac{H^{bt}_{\downarrow}(-p,t)}{H^{bt}_{\uparrow}(-p,t)}=e^{i(\psi_\uparrow-\psi_\downarrow+\pi)}.\quad \text{(B16)}$$

Finally, since $\Delta^{tb}_{\uparrow\downarrow}\propto\langle c_{t\uparrow}c_{b\downarrow}\rangle$, $\Delta^{tb}_{\uparrow\downarrow}=-\Delta^{bt}_{\downarrow\uparrow}$:

$$\frac{\bar{\Delta}^{bt}_{\uparrow\downarrow}}{\bar{\Delta}^{tb}_{\uparrow\downarrow}}=e^{i(\psi_\uparrow-\psi_\downarrow)}.\quad \text{(B17)}$$

Note that we did not imply anything about layer symmetry.

APPENDIX C: STABILITY OF THE PARALLEL PHASE

To explore the stability of the parallel state we first represent the original Hamiltonian in the basis of the symmetric/antisymmetric states

$$c_{+,\sigma}=\frac{1}{\sqrt{2}}(c_{t,\sigma}+c_{b,\sigma}),\quad \text{(C1)}$$

$$c_{-,\sigma}=\frac{1}{\sqrt{2}}(c_{t,\sigma}-c_{b,\sigma}),\quad \text{(C2)}$$

and perform the Bogolyubov transformation

$$c_{p\alpha\downarrow}=u^*_{\alpha p}\gamma_{\alpha-}(p)-v_{\alpha p}\gamma^\dagger_{\alpha+}(-p),\quad \text{(C3)}$$

$$c_{p\alpha\uparrow}=v_{\alpha p}\gamma^\dagger_{\alpha-}(-p)+u^*_{\alpha p}\gamma_{\alpha+}(p).\quad \text{(C4)}$$

Since we perform Bogolyubov rotation within symmetric and antisymmetric subspaces separately, there are only two parameters at each k-point. Condition for bogolyubons to be fermions is $|u_{\alpha k}|^2+|v_{\alpha k}|^2=1$. Rewriting energy in terms of angles $u_{\alpha k}=\cos(\theta_{\alpha k})$ and $v_{\alpha k}=\sin(\theta_{\alpha k})$ we obtain:

$$E=2\sum\xi_k\sin(\theta_{\alpha k})^2-\frac{\lambda_x}{2^3S}\Big(\sum[\cos(2\theta_{+k})-\cos(2\theta_{-k})]\Big)^2+\frac{\lambda_+}{2^2S}\sum\sin(2\theta_{\alpha k})\sin(2\theta_{\alpha k'})+\frac{\lambda_-}{2S}\sum\sin(2\theta_{+k})\sin(2\theta_{-k'}),\quad \text{(C5)}$$

where $\lambda_+=(\lambda_x+\lambda_s)/2$, $\lambda_-=(\lambda_s-\lambda_x)/2$. The self-energies become

$$\Delta_d=-\frac{\lambda_s}{S}\sum_{k'}\langle c_{t\uparrow}(k')c_{t\downarrow}(-k')\rangle=-\frac{\lambda_s}{2S}\sum_{k'\alpha}u^*_{\alpha k'}v_{\alpha k'}=-\frac{\lambda_s}{4S}\sum_{k'\alpha}\sin(2\theta_{\alpha k'}),\quad \text{(C6)}$$

$$\Delta_i=-\frac{\lambda_x}{S}\sum_{k'}\langle c_{t\uparrow}(k')c_{b\downarrow}(-k')\rangle=-\frac{1}{2S}\sum_{k'}\lambda_x u^*_{\alpha k'}v_{\beta k'}\tau^z_{\alpha\beta}=-\frac{\lambda_x}{4S}\sum_{k'}[\sin(2\theta_{+k})-\sin(2\theta_{-k})],\quad \text{(C7)}$$

$$x = \frac{\lambda_x}{S}\sum_{k'}\langle c^\dagger_{b\uparrow}(k')c_{t\uparrow}(k')\rangle$$
$$= -\frac{\lambda_x}{4S}\sum_k[\cos(2\theta_{+k}) - \cos(2\theta_{-k})]. \quad \text{(C8)}$$

Minimization of energy with respect to the Bogolyubov angles gives

$$\tan(2\theta_{k\pm}) = \frac{\lambda_+ S_\pm + \lambda_- S_\mp}{-\xi_k \pm x}, \quad \text{(C9)}$$

where $d_\pm = \frac{1}{2S}\sum_k \sin(2\theta_{\pm k})$ is the superconducting amplitude. Nondiagonal entries of the matrix of second-order derivatives vanish in the thermodynamic limit. Diagonal entries are

$$\frac{1}{2}\frac{\partial^2 E}{\partial\theta^2_{\pm k}} = \cos(2\theta_\pm)[(-\xi_k \pm x) + \tan(2\theta_\pm)(d_\pm\lambda_+ + \lambda_- d_\mp)]. \quad \text{(C10)}$$

At the energy extrema from (C9)

$$\frac{1}{2}\frac{\partial^2 E}{\partial\theta^2_{\pm k}} = \frac{\cos(2\theta_{\pm k})}{-\xi_k \pm x}[(\xi_k \pm x)^2 + (d_\pm\lambda_+ + \lambda_- d_\mp)^2]. \quad \text{(C11)}$$

The stability requires that $\frac{\partial^2 E}{\partial\theta^2_{\pm k}} \geqslant 0$ at any k-point. Using (C9) to express the $\cos(2\theta)$, we get

$$\frac{1}{2}\frac{\partial^2 E}{\partial\theta^2_{\pm k}} = \frac{1}{\sqrt{(\lambda_+ d_\pm + \lambda_+ d_\mp)^2 + (\xi_k \mp x)^2}} \times [(\xi_k \mp x)^2 + (d_\pm\lambda_+ + \lambda_- d_\mp)^2] > 0, \quad \text{(C12)}$$

we then conclude that both solutions ($f = 1, f = 0$) will be stable in the thermodynamic limit. Now we use the expression for energy to see if one of the solutions has lower energy than the other

$$E = \text{const.} - \sum_k \frac{(\xi_k - x)\xi_k}{\sqrt{(d_+\lambda_+ + \lambda_- d_-)^2 + (\xi_k - x)^2}} - \sum_k \frac{(\xi_k + x)\xi_k}{\sqrt{(d_-\lambda_+ + \lambda_- d_+)^2 + (\xi_k + x)^2}} - \frac{2x^2}{\lambda_x} + \frac{2\Delta_d^2}{\lambda_s} + \frac{2\Delta_i^2}{\lambda_x}. \quad \text{(C13)}$$

Let us isolate a part sensitive to a permutation of $\Delta_+ \equiv \Delta_d + \Delta_i$ and $\Delta_- \equiv \Delta_d - \Delta_i$. It reads

$$E_{\text{asym}} = x\nu\left(\int d\xi \frac{\xi - x}{\sqrt{\Delta_-^2 + (\xi - x)^2}} - \frac{\xi + x}{\sqrt{\Delta_+^2 + (\xi + x)^2}}\right). \quad \text{(C14)}$$

Most of the time we have a fully polarized solution $x = \mu$ and thus the contribution from the second term is always negative. The contribution from the first term is only negative for the range of energies between $-\mu$ and μ. If the high-energy energy cutoff $\Lambda > 2\mu$ we better have $\Delta_+ < \Delta_-$ to minimize the energy. We then conclude that $\Delta_i < 0$ or, in other words, the $f = 1$ solution has lower energy in accordance to our numerical calculations. We also see that, because the negative contribution from the first term is proportional to the $-\mu\nu\sqrt{\Delta_-^2 + (2\mu)^2}$, there could be be an energy benefit from having superconducting gaps larger than the one predicted through the Macmillan in the absence of the interlayer coherence. Additionally, let us clarify here the dependence of gaps on interaction parameters that follow from the gap equations (20) and (21). First, the exciton order parameter x acquires constant value μ almost immediately after the phase transition and that is why we will it ignore it with the functional dependence deep into the mixed phase. If $\lambda_x \gg |\lambda_s|$,

$$-\frac{1}{\lambda_s}(\Delta_+ + \Delta_-) \approx \frac{\Delta_+}{2}\int \frac{d\xi\,\nu(\xi)}{\sqrt{(\xi + x)^2 + \Delta_+^2}}, \quad \text{(C15)}$$

$$-\frac{1}{\lambda_s}(\Delta_- + \Delta_+) \approx \frac{\Delta_-}{2}\int \frac{d\xi\,\nu(\xi)}{\sqrt{(\xi - x)^2 + \Delta_-^2}}. \quad \text{(C16)}$$

Then for small Δ_-, Δ_+ it follows that $\Delta_+ \approx \Delta_-$ and thus $\Delta_i \approx 0$. Then it immediately follows that Δ_d does not depend on interaction between layers λ_x. Look now at the opposite limit $|\lambda_s| \gg \lambda_x$. In this case,

$$-\frac{1}{\lambda_x}(\Delta_+ - \Delta_-) \approx \frac{\Delta_+}{2}\int \frac{d\xi\,\nu(\xi)}{\sqrt{(\xi + x)^2 + \Delta_+^2}}, \quad \text{(C17)}$$

$$-\frac{1}{\lambda_x}(\Delta_- - \Delta_+) \approx \frac{\Delta_-}{2}\int \frac{d\xi\,\nu(\xi)}{\sqrt{(\xi - x)^2 + \Delta_-^2}}, \quad \text{(C18)}$$

from which we conclude that gaps depend only on g_x in this limit. Interestingly, such a solution would require $\Delta_d < \Delta_i$, which is nonphysical. In the intermediate regime $\lambda_x \approx |\lambda_s|$ we expect the gaps depend on the combination $\lambda_x - \lambda_s$, so that the gaps should be constant along the lines $g_s = g_x + C$.

[1] J. Bardeen, L. N. Cooper, and J. R. Schrieffer, Phys. Rev. **108**, 1175 (1957).
[2] J. Bardeen, L. N. Cooper, and J. R. Schrieffer, Phys. Rev. **106**, 162 (1957).
[3] A. Andreev, Sov. Phys. JETP **20**, 1490 (1965).
[4] D. Bradley, A. Guénault, R. Haley, G. Pickett, and V. Tsepelin, Annu. Rev. Condens. Matter Phys. **8**, 407 (2017).
[5] C. W. J. Beenakker, Rev. Mod. Phys. **80**, 1337 (2008).
[6] M. J. M. de Jong and C. W. J. Beenakker, Phys. Rev. Lett. **74**, 1657 (1995).
[7] M. Diez, J. P. Dahlhaus, M. Wimmer, and C. W. J. Beenakker, Phys. Rev. B **86**, 094501 (2012).
[8] C. W. J. Beenakker, Phys. Rev. Lett. **97**, 067007 (2006).
[9] J. Nilsson, A. R. Akhmerov, and C. W. J. Beenakker, Phys. Rev. Lett. **101**, 120403 (2008).

[10] T. D. Stanescu, R. M. Lutchyn, and S. Das Sarma, Phys. Rev. B **84**, 144522 (2011).
[11] A. Kundu and B. Seradjeh, Phys. Rev. Lett. **111**, 136402 (2013).
[12] I. I. Mazin, Phys. Rev. Lett. **83**, 1427 (1999).
[13] I. Mazin, A. A. Golubov, and B. Nadgorny, J. Appl. Phys. **89**, 7576 (2001).
[14] S. Sasaki, M. Kriener, K. Segawa, K. Yada, Y. Tanaka, M. Sato, and Y. Ando, Phys. Rev. Lett. **107**, 217001 (2011).
[15] A. Kastalsky, A. W. Kleinsasser, L. H. Greene, R. Bhat, F. P. Milliken, and J. P. Harbison, Phys. Rev. Lett. **67**, 3026 (1991).
[16] H. Pothier, S. Guéron, D. Esteve, and M. H. Devoret, Phys. Rev. Lett. **73**, 2488 (1994).
[17] W. K. Park, L. H. Greene, J. L. Sarrao, and J. D. Thompson, Phys. Rev. B **72**, 052509 (2005).
[18] X. Xi, Z. Wang, W. Zhao, J.-H. Park, K. T. Law, H. Berger, L. Forró, J. Shan, and K. F. Mak, Nat. Phys. **12**, 139 (2016).
[19] Y. Li, Q. Gu, C. Chen, J. Zhang, Q. Liu, X. Hu, J. Liu, Y. Liu, L. Ling, M. Tian *et al.*, Proc. Natl. Acad. Sci. **115**, 9503 (2018).
[20] Y.-T. Hsu, W. S. Cole, R.-X. Zhang, and J. D. Sau, Phys. Rev. Lett. **125**, 097001 (2020).
[21] A. D. K. Finck, J. P. Eisenstein, L. N. Pfeiffer, and K. W. West, Phys. Rev. Lett. **104**, 016801 (2010).
[22] P. Simonet, S. Hennel, H. Overweg, R. Steinacher, M. Eich, R. Pisoni, Y. Lee, P. Märki, T. Ihn, K. Ensslin *et al.*, New J. Phys. **19**, 103042 (2017).
[23] G. W. Burg, N. Prasad, K. Kim, T. Taniguchi, K. Watanabe, A. H. MacDonald, L. F. Register, and E. Tutuc, Phys. Rev. Lett. **120**, 177702 (2018).
[24] L. V. Keldysh and A. N. Kozlov, Sov. Phys. JETP **27**, 521 (1968).
[25] Y. E. Lozovik and V. Yudson, JETP Lett. **22**, 274 (1975).
[26] E. Hanamura and H. Haug, Phys. Rep. **33**, 209 (1977).
[27] P. Littlewood, P. Eastham, J. Keeling, F. Marchetti, B. Simons, and M. Szymanska, J. Phys.: Condens. Matter **16**, S3597 (2004).
[28] A. Perali, D. Neilson, and A. R. Hamilton, Phys. Rev. Lett. **110**, 146803 (2013).
[29] M. Fogler, L. Butov, and K. Novoselov, Nat. Commun. **5**, 4555 (2014).
[30] E. Fradkin, S. A. Kivelson, M. J. Lawler, J. P. Eisenstein, and A. P. Mackenzie, Annu. Rev. Condens. Matter Phys. **1**, 153 (2010).
[31] A. Kogar, M. S. Rak, S. Vig, A. A. Husain, F. Flicker, Y. I. Joe, L. Venema, G. J. MacDougall, T. C. Chiang, E. Fradkin *et al.*, Science **358**, 1314 (2017).
[32] Y. Mazuz-Harpaz, K. Cohen, M. Leveson, K. West, L. Pfeiffer, M. Khodas, and R. Rapaport, Proc. Natl. Acad. Sci. **116**, 18328 (2019).
[33] A. High, J. Leonard, M. Remeika, L. Butov, M. Hanson, and A. Gossard, Nano Lett. **12**, 2605 (2012).
[34] R. Bistritzer and A. H. MacDonald, Proc. Natl. Acad. Sci. **108**, 12233 (2011).
[35] Y. Cao, V. Fatemi, S. Fang, K. Watanabe, T. Taniguchi, E. Kaxiras, and P. Jarillo-Herrero, Nature (London) **556**, 43 (2018).
[36] F. Wu, A. H. MacDonald, and I. Martin, Phys. Rev. Lett. **121**, 257001 (2018).
[37] B. Lian, Z. Wang, and B. A. Bernevig, Phys. Rev. Lett. **122**, 257002 (2019).
[38] V. Kozii, H. Isobe, J. W. F. Venderbos, and L. Fu, Phys. Rev. B **99**, 144507 (2019).
[39] D. V. Chichinadze, L. Classen, and A. V. Chubukov, Phys. Rev. B **101**, 224513 (2020).
[40] E. Khalaf, S. Chatterjee, N. Bultinck, M. P. Zaletel, and A. Vishwanath, Sci. Adv. **7**, eabf5299 (2021).
[41] Y. Cao, V. Fatemi, A. Demir, S. Fang, S. L. Tomarken, J. Y. Luo, J. D. Sanchez-Yamagishi, K. Watanabe, T. Taniguchi, E. Kaxiras *et al.*, Nature (London) **556**, 80 (2018).
[42] X. Lu, P. Stepanov, W. Yang, M. Xie, M. A. Aamir, I. Das, C. Urgell, K. Watanabe, T. Taniguchi, G. Zhang *et al.*, Nature (London) **574**, 653 (2019).
[43] M. Yankowitz, S. Chen, H. Polshyn, Y. Zhang, K. Watanabe, T. Taniguchi, D. Graf, A. F. Young, and C. R. Dean, Science **363**, 1059 (2019).
[44] J. M. Park, Y. Cao, K. Watanabe, T. Taniguchi, and P. Jarillo-Herrero, Nature (London) **590**, 249 (2021).
[45] P. Rickhaus, F. de Vries, J. Zhu, E. Portolés, G. Zheng, M. Masseroni, A. Kurzmann, T. Taniguchi, K. Wantanabe, A. H. MacDonald *et al.*, Science **373**, 1257 (2021).
[46] L. M. Sager, S. Safaei, and D. A. Mazziotti, Phys. Rev. B **101**, 081107(R) (2020).
[47] S. Conti, A. Perali, F. M. Peeters, and D. Neilson, Phys. Rev. Lett. **119**, 257002 (2017).
[48] A. A. Vargas-Paredes, A. A. Shanenko, A. Vagov, M. V. Milošević, and A. Perali, Phys. Rev. B **101**, 094516 (2020).
[49] J.-J. Su and A. MacDonald, Nat. Phys. **4**, 799 (2008).
[50] X. Liu, K. Watanabe, T. Taniguchi, B. I. Halperin, and P. Kim, Nat. Phys. **13**, 746 (2017).
[51] J. Eisenstein, Annu. Rev. Condens. Matter Phys. **5**, 159 (2014).
[52] Y. Yoon, L. Tiemann, S. Schmult, W. Dietsche, K. von Klitzing, and W. Wegscheider, Phys. Rev. Lett. **104**, 116802 (2010).
[53] J. Li, T. Taniguchi, K. Watanabe, J. Hone, and C. Dean, Nat. Phys. **13**, 751 (2017).
[54] J. Li, Q. Shi, Y. Zeng, K. Watanabe, T. Taniguchi, J. Hone, and C. Dean, Nat. Phys. **15**, 898 (2019).
[55] One way to represent these quantities is to imagine a space with four points corresponding to each kind of fermion. Then any gauge-invariant quantity will correspond to a closed trajectory between these points.
[56] The condition written assuming all three order parameters Σ, Δ, and x are nonzero. If $\Sigma = 0$, ψ_+ can be any.
[57] G. Blonder, m. M. Tinkham, and K. T. Klapwijk, Phys. Rev. B **25**, 4515 (1982).
[58] D. M. Kennes, M. Claassen, L. Xian, A. Georges, A. J. Millis, J. Hone, C. R. Dean, D. Basov, A. N. Pasupathy, and A. Rubio, Nat. Phys. **17**, 155 (2021).
[59] M. Xie and A. H. MacDonald, Phys. Rev. Lett. **127**, 196401 (2021).